Published by
NIGERIAN SOCIETY OF PHYSICAL SCIENCES
Available online @ https://journal.nsps.org.ng/index.php/jnsps

J. Nig. Soc. Phys. Sci. 7 (2025) 2309

Journal of the Nigerian Society of Physical Sciences

Green synthesis of CuO nanoparticles from *Cucurbita maxima* leaf extract; a platinum free counter electrode for dye sensitized solar cells

Emma Panzi Mukhokosi[a,*], Stephen Tenywa[a], Nandipha L. Botha[b,c], Shohreh Azizi[b,c], Mathapelo Pearl Seopela[d], Malik Maaza[b,c]

[a]*Department of Physics, Faculty of Science, Kyambogo University, PO Box 1, Kampala, Uganda*
[b]*College of Graduate Studies, UNESCO UNISA Africa Chair in Nanosciences & Nanotechnology, University of South Africa, Pretoria, South Africa*
[c]*Materials Research Department, Nanosciences African Network (NANOAFNET), iThemba LABS, PO Box 722, Cape Town, South Africa*
[d]*Department of Chemical Sciences, University of South Africa, Auckland Park Campus, PO Box 524, Auckland Park, 2006, Johannesburg, South Africa*

Abstract

Green synthesis of metal oxides has attracted attention as the latest technology in synthesizing metal oxide nanoparticles due to its simplicity, cheapness, non-toxicity and its ability for large scale production. Metal oxides find applications in dye sensitized solar cells (DSSCs) as counter electrodes (CEs) and photo-anodes. However, applications of green synthesized metal oxides as counter electrodes have not been fully explored. In this study, CuO nanoparticles (NPs) were synthesized from *Cucurbita maxima* leaf extract and applied as a CE in DSSC. Uniformly synthesized CuO NPs were subjected to various characterization tools to obtain the crystal structure, surface morphology, particle size, optical properties, chemical bonds and photovoltaic properties. Using a natural dye from of *Cucurbita maxima* as a photon absorber, a short circuit current density (J_{sc}) of 4.2 μA/cm^2, open circuit voltage (V_{oc}) of 0.17 V, a maximum power (P_{max}) of 0.18 mW/cm^2, and a power conversion efficiency (PCE) of 1.8×10^{-4} % under one-sun illumination were obtained.

DOI:10.46481/jnsps.2025.2309

Keywords: Green synthesis, DSSCs, CuO, Cucurbita maxima, Natural dye

Article History :
Received: 13 August 2024
Received in revised form: 25 October 2024
Accepted for publication: 29 October 2024
Available online: 15 December 2024

Communicated by: B. J. Falaye

1. Introduction

Energy is a crucial component in all sectors of countries as it facilitates economic transformation and development. Clean and sustainable energy is vital so as to realize the United Nations Sustainable Development Goals (SDGs) [1]. DSSCs are a third-generation photovoltaic devices which are being researched as a prospective replacement to first and second generational solar cells. Their wide spread research interest is attributed to their simple device architecture, easy to fabricate, less toxicity and comparatively high power conversion efficiency. The current PCE of DSSCs is reported at 14.7% [2]. The basic components of a DSSC are a photoanode, a dye sensitizer and a counter electrode (CE). Platinum (Pt) has mainly been used as an efficient CE due to its excellent catalytic ac-

*Corresponding author: Tel.: +0-000-000-0000.
Email address: panzi2018@gmail.com (Emma Panzi Mukhokosi)

tivity and stability [3–6]. However, it is scarce and expensive. Various efforts have therefore been directed towards developing Pt free CEs with equal or higher catalytic activity for DSSCs. Such alternatives have to be affordable and should exhibit all advantages of platinum characteristics for DSSC applications. The possible CE alternatives are metal composites, nitrides, carbides, metal oxides, 2D-Transitional metal dichalcogenides, conducting polymers and carbon related materials such as graphene, carbon nanotubes, reduced graphene oxide and carbon black [7–13]. Among these alternatives, metal oxides are simple to process and are abundant in the earth's crust. The metal oxides have demonstrated the PCE of similar or higher levels compared to Pt electrodes [14–17]. Both physical and chemical methods have conventionally been used to synthesize metal oxide NPs. However, the conventional techniques are expensive and involve the use of toxic and environmentally non friendly materials [18–22]. Among the oxides, CuO has attracted research attention due to its good electrical conductivity, excellent catalytic and antibacterial properties, with diverse applications in gas sensors, batteries, catalysis, field emission devices and photovoltaic devices [23–27]. In an effort to find an alternative cheaper, environmentally, and non-toxic technique for metal oxide synthesis, green synthesis is considered as the best option [28–36]. In addition, this method is straight forward, and produces stable NPs quickly by just adjusting the pH and annealing temperature [21, 37–41]. CuO NPs of different particle sizes, surface morphologies and dimensions have been synthesized from different plant materials for antibacterial, antimicrobial, and photocatalytic applications and have rarely been investigated for applications as CEs in DSSCs [28–31, 33]. It can further be noted that different plant materials have different bioactive compounds that can reduce metal salts to NPs of various morphologies, size and dimensions. For instance, *Cucurbita maxima* leaf contain phenol, flavonoids, alkaloids, tannin, saponin, terpenoids and steroids as bio active compounds [42]. For DSSCs applications, Sharma *et al*. [36], synthesized a 20 nm spherically shaped CuO NPs from leaf extract of *Calotropis gigantea* and they fabricated a CE for DSSCs. Using a synthetic dye, a fill factor (FF) of 0.62, a J_{sc} of 8.13 mA/cm^2, a PCE of 3.4 % and an V_{oc} of 0.676 V were obtained. Therefore, further research on green synthesis of CuO by other plant materials needs to investigated. In this article, spherically shaped CuO NPs of < 10 nm in particle size were synthesized from *Cucurbita maxima* leaf extract and applied as a CE in DSSC. Using a natural dye from of *Cucurbita maxima* as a photon absorber, a J_{sc} of 4.2 μA/cm^2, V_{oc} of 0.17 V, P_{max} of 0.18 mW/cm^2, and a PCE of 1.8×10^{-4} % under one-sun illumination were obtained.

2. Materials and Methods

2.1. Materials

The materials used were; Cupric nitrate, ethanol, polyethylene glycol (PEG), anhydrous titanium oxide powder, iodide/triiodide electrolyte, Fluorine doped tin oxide (FTO) coated glass substrate of sheet resistance = 6.7 ± 0.27 Ω/square

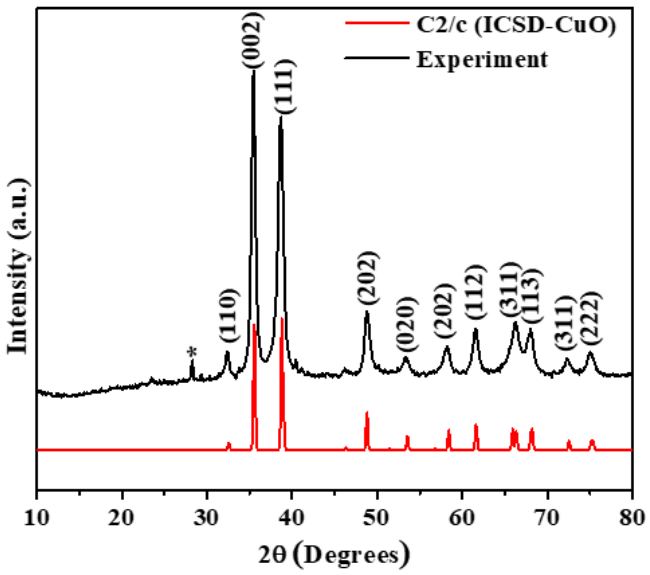

Figure 1. XRD pattern of CuO NPs.

cm from Ossila Ltd-UK and distilled water. TiO_2 powder < 25 nm (anatase phase). All chemicals were obtained from Sigma Aldrich and were used without further purifications. *Cucurbita maxima* plant leaves were obtained from Ugandan.

2.2. Plant Extract Preparation

Fresh leaves of *Cucurbita maxima* were cleaned twice using distilled water and dried under the sun. The dried leaves were ground using a mortar and pestle to form a powder. 500 mL of distilled water was mixed with 50 g of the powder, the mixture was placed on a hot plate and heated at 70 °C for 1 hour. The solution was then sieved twice using Whatman filter paper (Cat No 1001 125) to eliminate any residual solids.

2.3. Synthesis of CuO nanoparticles

50 mL of the leaf extract was mixed with 2.5 g of cupric nitrate in a beaker, the mixture was placed a hot plate at 70 °C and uniformly stirred using a magnetic stirrer for 1 hour. A yellowish-green colored solution was observed. The resultant solution was placed in an oven at 100 °C for 18 h and a pale green powder of CuO was obtained. To crystallize CuO, the powder was placed in a ceramic crucible and calcinated between 350 and 450 °C for 2 h. The choice of annealing temperature was based on previous literature [29, 34].

2.4. Preparation of the dye solutions for use as photosensitizers.

We used a natural dye of *Cucurbita maxima* leaf extract, the extraction procedures and optical absorption properties of the dye are reported elsewhere [43, 44].

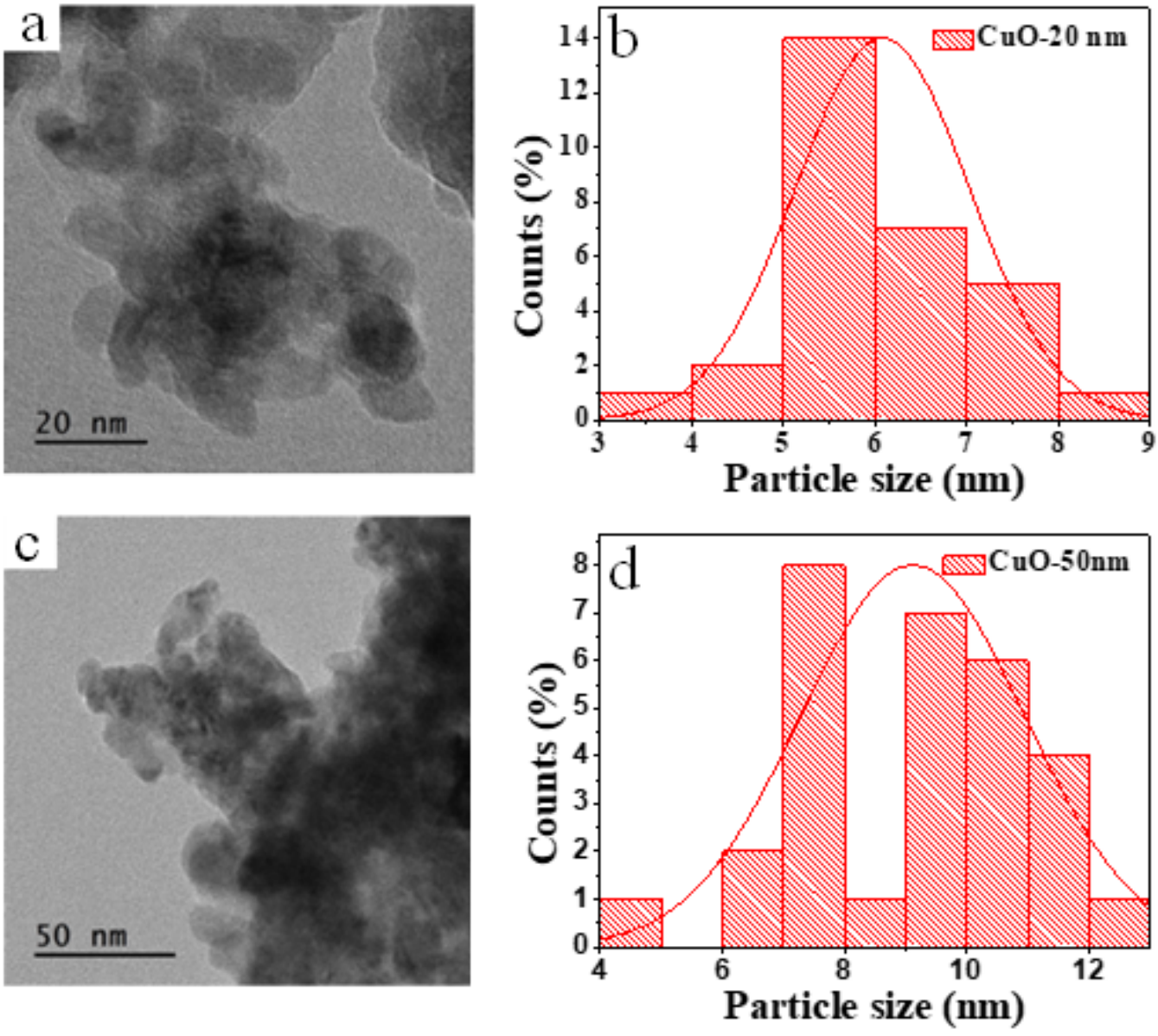

Figure 2. (a) TEM image for CuO NPs at calcinated at 350 °C, (b) TEM image for CuO NPs calcinated at 450 °C, (c) Histogram for particle size distribution for sample calcinated at 350 °C and (d) Histogram for particle distribution for sample calcinated at 450 °C.

2.5. *Preparation of the electrodes*

2.5.1. *Substrate cleaning*

The FTO glass substrates of dimensions 2.5 cm × 2.5 cm were rinsed with distilled water followed by ethanol for 30 minutes in an ultrasonic bath. They were then dried in an oven at 60 °C for 15 minutes. The edges of the substrates were covered with a scotch tape of thickness 0.06 mm.

2.5.2. *Fabrication of counter electrode*

0.2 g of CuO powder was mixed in a solution containing 0.4 g of polyethylene glycol (PEG) binder, 5 milliliters of acetic acid and 5 milliliters distilled water. The resultant mixture was sonicated for 2 h and then spin coated five times at 2500 rotations per minute (rpm) for 10 minutes. The choice of the spin coating speed was based on the theoretical understanding that high spin rate of 2500 rpm results in fast drying, formation of thinner and uniform thin film [45]. The thin film was kept in a clean environment for 24 h and left to dry. To remove the binder, solvent and grow the thin film on the substrate, the thin film was annealed at 300 °C for 1 h [46]. After cooling naturally, the annealed thin film was removed and kept in a clean environment for further use.

2.5.3. *Fabrication of Photoanode*

1 g of TiO_2 powder was mixed with 0.4 g of PEG binder in a solution containing 5 milliliters glacial acetic acid and 5 milliliters of distilled water. The resultant mixture was sonicated for 2 h and then spin coated five times each at 2500 rpm

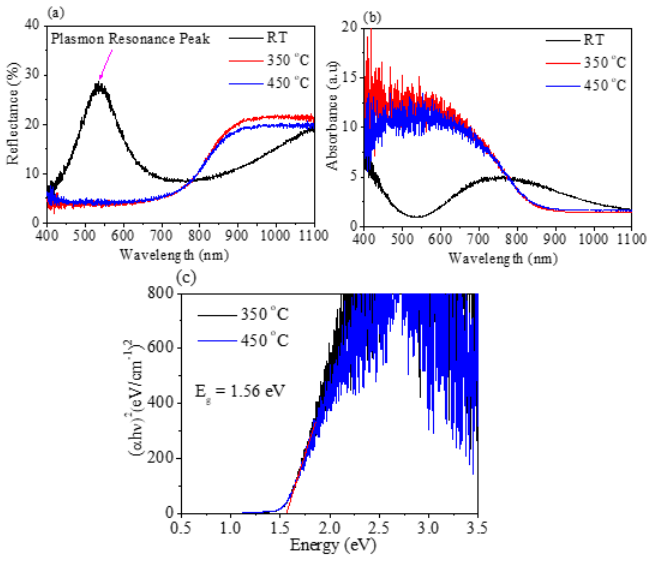

Figure 3. (a) Reflectance versus wavelength of CuO NPs at different temperatures, (b) Absorbance versus wavelength for CuO NPs at different temperatures and (c) Tauc plot for CuO NPs at 350 and 450 °C.

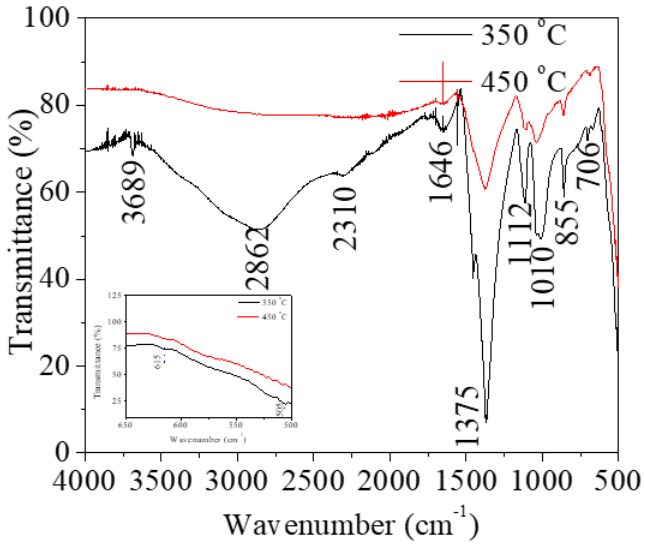

Figure 4. FTIR spectra for CuO nanoparticles annealed at 350 and 450 °C.

for 10 minutes on a pre-cleaned FTO substrate. The thin film was then annealed in a muffle furnace at 300 °C for 1 h. The furnace was left to cool naturally to room temperature. The TiO_2 thin film was removed and immersed in the dye extract for 24 hours. The soaked thin film was removed from the dye extract, rinsed with ethanol and kept in a clean environment for further use.

2.6. *Preparation of liquid electrolyte*

0.127 g of Iodine (I_2) and 0.83 g of potassium iodide (KI) were dissolved in 10 ml ethylene glycol, stirred for 30 min, kept in glass bottle for further use as an electrolyte [44, 47].

2.7. *Characterization methods*

The crystal structurer of CuO nanoparticles were investigated using X-ray diffractometer (XRD) (Cu-Kα radiation, λ = 1.5418 Å) [48]. The surface morphology and particle size of CuO NPs were evaluated using a Transmission Electron Microscope (TEM) [43]. The optical properties of CuO NPs were investigated using a UV–visible–NIR spectrophotometer [49]. The functional groups in CuO NPs were investigated using a Fourier Transform Infrared (FTIR) Spectrophotometer (IR Tracer 100, Equipment no. A21705601203).

2.8. *Assembly of DSSC and current-voltage (I-V) measurements*

The TiO_2 photo-anode and CuO counter electrode were sandwiched together with the conductive sides facing each other. A few drops of the electrolyte were drawn into the space between the electrodes by capillary action. The electrodes were firmly held together using binder clips. The device was illuminated with a solar simulator under standard conditions (AM1.5 100 $mWcm^{-2}$) and the *I-V* characteristic were recorded using Keithley SMU-2450 [44]. The active area of the device was 4.0 cm^2.

3. Results and discussion

The diffraction data was compared with standard data from files of the Inorganic Crystal Structure Database (ICSD) of space group C2/c (ICSD number 16025) and was indexed. Figure 1 shows the XRD pattern of CuO NPs and its corresponding ICSD data. The extra peak at 28.3° is due to the impurity phase of Cu $(OH)_2$. The average crystallite size (D) of the CuO NPs was estimated according to the Debye-Scherer;

$$D = \frac{K\lambda}{\beta Cos\theta}, \tag{1}$$

where, K is Scherer constant, taken as 0.9, λ =1.5418 Å is the X-ray wavelength, θ is diffraction angle and β is the full width at half maximum (FWHM) intensity. The dislocation density (δ) and micro strain (ε) were evaluated using equations (2) and (3) respectively.

$$\delta = \frac{1}{D^2}, \tag{2}$$

$$\frac{\beta Cos\theta}{4}, \tag{3}$$

the values of D, ε and δ are computed as shown in Table 1.

The average values were D = 10.8 nm, ε = 0.367 % and δ = 1.26×10^{-4} line/m^2 respectively. Figures 2a and 2b shows the TEM image of CuO NPs and its histogram for particle size distribution at calcination temperatures of 350 °C. Figures 2c and 2d shows TEM image of CuO NPs and its histogram for particle size distribution at synthesis temperature of 450 °C. The images reveal that CuO NPs are spherically shaped and agglomerated.

Table 1. Results for XRD analysis of CuO NPs.

Peak	(2θ) (°)	(hkl)	β (Radians)	D (Å)	ε (%)	δ (line/m^2)
1	32.4	110	0.564	147	0.236	4.63×10^{-5}
2	35.5	002	0.607	138	0.252	5.29×10^{-5}
3	38.7	111	0.841	100	0.346	9.95×10^{-5}
4	48.8	202	0.716	122	0.284	6.71×10^{-5}
5	53.4	020	1.115	80	0.432	1.55×10^{-4}
6	58.3	202	0.733	124	0.279	6.48×10^{-5}
7	61.6	113	0.727	127	0.272	6.16×10^{-5}
8	66.2	311	1.363	70	0.498	2.06×10^{-4}
9	68.0	113	0.952	101	0.344	9.85×10^{-5}
10	72.4	311	0.901	109	0.317	8.37×10^{-5}
11	75.0	222	1.086	92	0.375	1.17×10^{-4}

The average particle size at calcination temperature of 350 and 450 °C were 6.1 ± 0.1 and 9.1 ± 0.1 nm respectively and are comparable to XRD crystallite size calculated in Table 1. The increase in particle size is thermodynamically influenced by the increase in temperature. In general, the particle size of CuO NPs realized in this article is smaller compared to previous reports [25, 36, 38, 50].

3.1. Optical properties of CuO nanoparticles

Figure 3a shows the diffuse reflection spectra (DRS) of CuO NPs for the as synthesized sample, calcinated sample at 350 and 450 °C. A sharp peak is observed at 536 nm for the as synthesized sample. The peak disappears with the increase in calcination temperature. The disappearance of the peak is attributed to phase transformation at 350 °C, which stabilizes at 450 °C and forms particle sizes above the resonance frequency [51]. The sharp peak at RT is attributed to surface Plasmon resonance absorption of metal oxide NPs, which is normally observed when the wavelength is greater than the particle size on the material [51, 52]. The DRS was converted to an equivalent absorption spectrum shown in Figure 3b using the Kubelka-Munk (KM) function [53]. The KM function is given by equation (4).

$$F(R) = \frac{K}{S} = \frac{(1-R)^2}{2R}, \tag{4}$$

where F(R) is the Kubelka Munk function that is the ratio of absorption coefficient K, to scattering coefficient S and R is reflectance.

The band gap was computed by making a Tauc plot given by equation (5):

$$(F(R)hv)^r = A\,(hv)\,, \tag{5}$$

where hv is the optical energy, A is a constant and r is equal to 2 if the transition is direct or 1/2 if the transition is indirect. The bandgap energy (E_g) of CuO NPs were obtained by extrapolating the linear parts of the graphs. Figure 3c shows the Tauc plot for CuO NPs at calcination temperatures of 350 and 450 °C. A band gap of 1.56 eV was estimated for both samples. The E_g values are higher than that of bulk CuO (E_g=1.2 eV [23]). The increase in E_g can be attributed to quantum size effects in nanomaterials [53–56].

3.2. Fourier Transform Infrared (FTIR) analysis

Figure 4 shows the FTIR Spectra CuO NPs at two calcination temperatures. A sharp peak at 3689 cm^{-1} is assigned to the asymmetric stretching of the O-H bond in alcohols [50, 57]. The broad band at 2862 cm^{-1} is due to the symmetric stretching of C–H bond [50]. The peak at 2310 cm^{-1} is due to C=O stretch and indicates the presence of alkanes [38]. A peak at 1646 cm^{-1} is assigned to C-C bond and shows the presence of alkenes [38]. The peak at 1357 cm^{-1} is assigned to C-N bond and indicates the presence of amine groups [50]. A peak located at 1112 cm^{-1}is due to Cu–OH bond [40] and the peak at 1010 cm^{-1} is assigned to CuO bond [57]. A vibration band at 855 cm^{-1} is assigned to –CH bending vibration [40]. A vibration band at 706 cm^{-1} is attributed to alcohol and phenolic groups, C–N stretching in amines [58]. Vibration bands at 615 cm^{-1} and 505 cm^{-1} in the inset of Figure 4 are assigned to the presence of CuO vibration bonds [36, 40, 50, 59].

4. Device J-V Analysis

Figure 5a and 5b shows the J-V and P-V characteristics of the fabricated solar cell. The power conversion efficiency (PCE) was evaluated using equation (6).

$$PCE = \frac{P_{max}}{P_{in}}\times100, \tag{6}$$

where P_{max} is the maximum power generated by the solar cell and P_{in} is the incident power density of the solar simulator (100 mW/cm^2). The solar cell yielded a PCE of 1.8×10^{-4} % with a J_{sc} of 0.18 μA cm^{-2} and V_{oc} of 0.17 V. The performance of the fabricated solar cell is low as compared to other metal oxide counter electrodes with Ruthenium based dye sensitizer [60–64]. However, the performance is comparable to other non-platinum counter electrodes with natural dye as sensitizers photon absorbers [64, 65]. Table 2 provides a summary of the performance of Pt and non-Pt CEs based DSSCs with natural dyes as photon absorbers. The efficiency of the fabricated device is 2 orders of magnitude lower than that of Pt and of the same order as other non-Pt CEs like carbon and carbon soot. In general, solar cells fabricated using natural dye sensitizers generally have

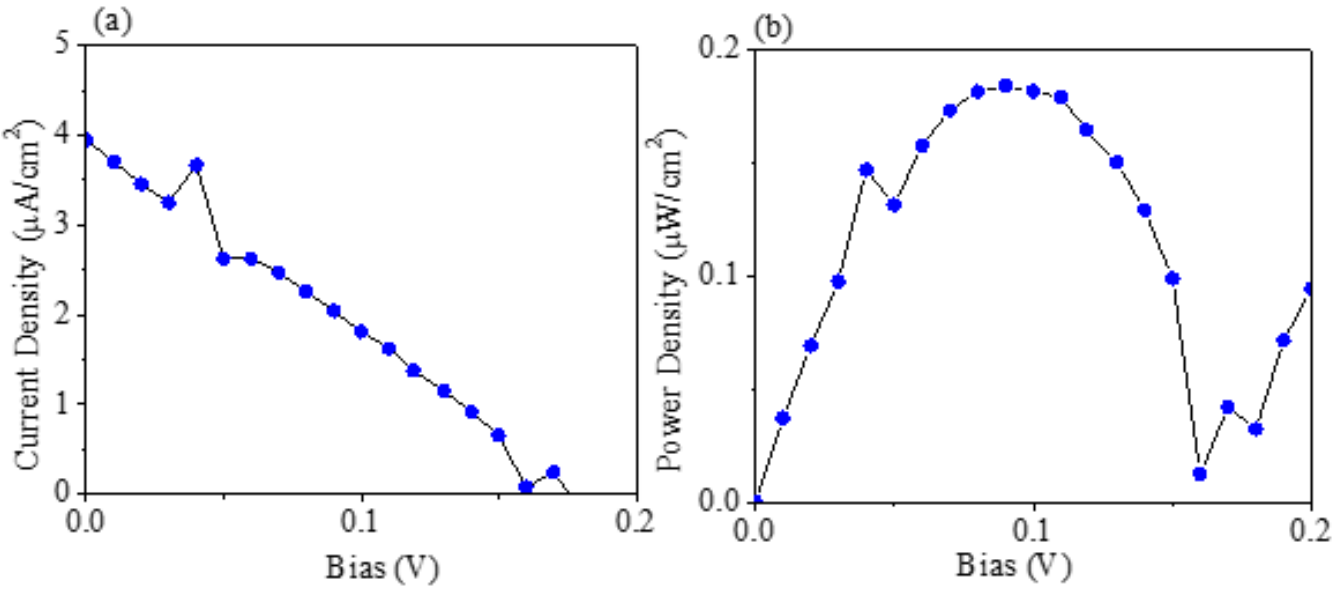

Figure 5. (a) *J-V* and (b) *P-V* characteristic curves of the device.

Table 2. Comparison of efficiency values for some few selected DSSCs based on natural dyes.

Counter electrode	Dye	PCE (%)	Reference
Pt	Strobilanthes cusia	1.18×10^{-2}	[68]
Pt	Ocimum Gratissimum	2.1×10^{-2}	[69]
Graphite	Strobilanthes cusia	3.85×10^{-2}	[68]
Carbon	Brassica oleracea var	$5.4E\times10^{-2}$	[70]
Carbon	Turmeric	2.0×10^{-3}	[71]
Carbon soot	Mangifera indica	2.35×10^{-4}	[65]
Carbon soot	Manihot esculenta	2.35×10^{-5}	[65]
CuO	Pumpkin leaves	1.8×10^{-4}	This study

low efficiency values, which is attributed to inefficient transfer of electrons into the conduction band of TiO_2 as compared to the commercial ruthenium based dyes sensitizers [66, 67].

5. Conclusion

In this study, CuO NPs of < 10 nm in particle size were synthesized using a cheap, simple and eco-friendly approach. The structural properties revealed a monoclinic phase of space group C2/c. The optical properties revealed a band gap of 1.56 eV for the calcinated samples. The DSSC revealed a PCE of 1.8×10^{-4} % with an open circuit voltage of 0.17 V, short circuit current density of 0.18 μA cm^{-2} and maximum power (P_{max}) of 0.18 mW/cm^2 under standard test conditions. Although this strategy for synthesizing CuO NPs using a green synthesis technique was successful, the power conversion efficiency of the solar cell was much lower as compared to conventional Platinum counter electrode [44]. Further studies on thickness control and other alternative thin film deposition technique such as dip-coating can possibly improve the efficiency of the DSSC cell using CuO as a counter electrode. In addition, other plant materials can be investigated to synthesize CuO nanoparticles of different dimensions. Further studies on the use of a standard ruthenium dye sensitizer, oxidation states of CuO using X-ray photoelectron spectroscopy, charge transfer resistance/dynamics and band alignments at the interface can enhance understanding of the synthesized material.

Acknowledgment

This research was financially supported by Kyambogo University Competitive Research Grants, The World Academy of Sciences, United Nations Educational Scientific and Cultural Organisation (TWAS-UNESCO)-Associateship Scheme at the Centres of Excellence in the South fellowship program, the United Nations Educational, Scientific and Cultural Organisation-University of South Africa (UNESCO-UNISA) Africa, Chair in Nanosciences & Nanotechnology and the Nano-sciences African Network (NANOAFNET). We thank the College of Science, Engineering and Technology at the University of South Africa for using the Rigaku SmartLab X-ray

diffractometer, which provided the measurements for the XRD patterns.

Data availability

The datasets generated during and/or analysed during the current study are available at https://drive.google.com/drive/u/0/folders/1lyZGRI1CWvsOIy32ZO056MA5wa3YkGWP.

References

[1] A. Pueyo & M. Maestre, "Linking energy access, gender and poverty: A review of the literature on productive uses of energy", Energy Research & Social Science **53** (2019) 170. https://doi.org/10.1016/j.erss.2019.02.019.

[2] K. Kakiage, Y. Aoyama, T. Yano, K. Oya, J.I. Fujisawa & M. Hanaya, "Highly-efficient dye-sensitized solar cells with collaborative sensitization by silyl-anchor and carboxy-anchor dyes", Chemical communications **51** (2015) 15894. https://doi.org/10.1039/c5cc06759f.

[3] S. A. Mahadik, H. M. Yadav & S. S. Mahadik, "Surface properties of chlorophyll-a sensitized TiO2 nanorods for dye-sensitized solar cells applications", Colloid and Interface Science Communications **46** (2022) 100558. https://doi.org/10.1016/j.colcom.2021.100558.

[4] K. Magiswaran, M. N. Norizan, N. Mahmed, I. S. Mohamad, S. N. Idris, M. F. M. Sabri, N. Amin, A. V. Sandu, P. Vizureanu, M. Nabiałek & M. A. A. M. Salleh, "Controlling the Layer Thickness of Zinc Oxide Photoanode and the Dye-Soaking Time for an Optimal-Efficiency Dye-Sensitized Solar Cell", Coatings **13** (2023) 20. https://doi.org/10.3390/coatings13010020.

[5] V. M. Mwalukuku, J. Liotier, A. J. Riquelme, Y. Kervella, Q. Huaulmé, A. Haurez, S. Narbey, J.A. Anta & R. Demadrille, "Strategies to improve the photochromic properties and photovoltaic performances of naphthopyran dyes in dye-sensitized solar cells", Advanced Energy Materials **13** (2023) 2203651. https://doi.org/10.1002/aenm.202203651.

[6] A. M. B. Leite, H. O. da Cunha, A. F. C. R. Rodrigues, R. Suresh Babu & A. L. F. de Barros, "Construction and characterization of organic photovoltaic cells sensitized by Chrysanthemum based natural dye", Spectrochim. Spectrochimica Acta Part A: Molecular and Biomolecular Spectroscopy **284** (2023) 121780. https://doi.org/10.1016/j.saa.2022.121780.

[7] A. R. Tapa, W. Xiang & X. Zhao, "Metal chalcogenides (MxEy; E = S, Se, and Te) as counter Electrodes for dye–sensitized solar cells: An overview and guidelines", Advanced Energy and Sustainability Research **10** (2021) 2100056. https://doi.org/10.1002/aesr.202100056.

[8] C. Gao, Q. Han & M. Wu, "Review on transition metal compounds based counter electrode for dye-sensitized solar cells", Journal of Energy Chemistry **27** (2018) 703. https://doi.org/10.1016/j.jechem.2017.09.003.

[9] E. Singh, K. S. Kim, G. Y. Yeom & H.S. Nalwa, "Two-dimensional transition metal dichalcogenide-based counter electrodes for dye-sensitized solar cells", RSC Advances **7** (2017) 28234. https://doi.org/10.1039/c7ra03599c.

[10] W. J. Lee, E. Ramasamy, D. Y. Lee & J. S. Song, "Performance variation of carbon counter electrode based dye-sensitized solar cell", Solar Energy Materials and Solar Cells **92** (2008) 814. https://doi.org/10.1016/j.solmat.2007.12.012.

[11] C. S. Wu, T. W. Chang, H. Teng & Y. L. Lee, "High performance carbon black counter electrodes for dye-sensitized solar cells", Energy **115** (2016) 513. https://doi.org/10.1016/j.energy.2016.09.052.

[12] X. Chen, J. Ding, Y. Li, Y. Wu, G. Zhuang, C. Zhang, Z. Zhang, C. Zhu & P. Yang, "Size-controllable synthesis of NiCoSe2 microspheres as a counter electrode for dye-sensitized solar cells", RSC Advances **8** (2018) 26047. https://doi.org/10.1039/c8ra04091e.

[13] R. Sankar Ganesh, K. Silambarasan, E. Durgadevi, M. Navaneethan, S. Ponnusamy, C. Y. Kong, C. Muthamizhchelvan, Y. Shimura & Y. Hayakawa, "Metal sulfide nanosheet–nitrogen-doped graphene hybrids as low-cost counter electrodes for dye-sensitized solar cells", Applied Surface Science **480** (2019) 177. https://doi.org/10.1016/j.apsusc.2019.02.251.

[14] S. Yun, L. Wang, W. Guo & T. Ma, "Non-Pt counter electrode catalysts using tantalum oxide for low-cost dye-sensitized solar cells", Electrochemistry communications **24** (2012).3 https://doi.org/10.1016/j.elecom.2012.08.008.

[15] J. Wu, Z. Lan, J. Lin, M. Huang, Y. Huang, L. Fan, G. Luo, Y. Lin, Y. Xie & Y. Wei, "Counter electrodes in dye-sensitized solar cells", Chemical Society Reviews **46** (2017) 5975. https://doi.org/10.1039/c6cs00752j.

[16] P. Jin, X. Zhang, M. Zhen & J. Wang, "MnO2 nanotubes with graphene-assistance as low-cost counter-electrode materials in dye-sensitized solar cells", RSC Advances **6** (2016) 10938. https://doi.org/10.1039/c5ra26995d.

[17] F. Du, Q. Yang, T. Qin & G. Li, "Morphology-controlled growth of NiCo2O4 ternary oxides and their application in dye-sensitized solar cells as counter electrodes", Solar Energy **146** (2017) 125. https://doi.org/10.1016/j.solener.2017.02.025.

[18] O. P. Keabadile, A. O. Aremu, S. E. Elugoke & O. E. Fayemi, "Green and traditional synthesis of copper oxide nanoparticles—comparative study", Nanomaterials **10** (2020) 2502. https://doi.org/10.3390/nano10122502.

[19] S. Saif, A. Tahir, T. Asim & Y. Chen, "Plant mediated green synthesis of CuO nanoparticles: Comparison of toxicity of engineered and plant mediated CuO nanoparticles towards Daphnia magna", Nanomaterials **6** (2016) 205. https://doi.org/10.3390/nano6110205.

[20] V. Selvanathan, M. Aminuzzaman, L. H. Tey, S. A. Razali, K. Althubeiti, H. I. Alkhammash, S. K. Guha, S. Ogawa, A. Watanabe, M. Shahiduzzaman & M. Akhtaruzzaman, "Muntingia calabura leaves mediated green synthesis of cuo nanorods: Exploiting phytochemicals for unique morphology", Materials **14** (2021) 6379. https://doi.org/10.3390/ma14216379.

[21] S. L. Valan, A. E. De Cruz, P. J. Jacob & S. Djearamane, "Sustainable synthesis of copper oxide nanoparticles using Aquilaria malaccensis (Agarwood) leaf extract as reducing Agent", International Journal of Technology **13** (2022) 1115. https://doi.org/10.14716/ijtech.v13i5.5845.

[22] Y. Bin Chan, V. Selvanathan, L. H. Tey, M. Akhtaruzzaman, F. H. Anur, S. Djearamane, A. Watanabe & M. Aminuzzaman, "Effect of calcination temperature on structural, morphological and optical properties of copper oxide nanostructures derived from Garcinia mangostana L. leaf extract", Nanomaterials **12** (2022) 3589. https://doi.org/10.3390/nano12203589.

[23] H. E. A. Mohamed, T. Thema & M. S. Dhlamini, "Green synthesis of CuO nanoparticles via Hyphaene thebaica extract and their optical properties", Materials Today : Proceedings **36** (2021) 591. https://doi.org/10.1016/j.matpr.2020.05.592.

[24] D. S. Hanafiah, G. Rakasiwi, E. I. M. Ibrahim, A. A. Abdelbagi, M. Magdalena, A. Noerdin & D. J. Indrani, "Green synthesis, characterization and antimicrobial activity of CuO nanoparticles (NPs) derived from Hibiscus sabdariffa a plant and CuCl", Journal of Physics: Conference Series" **1963** (2021) 012092. https://doi.org/10.1088/1742-6596/1963/1/012092.

[25] D. Das, B. C. Nath, P. Phukon & S. K. Dolui, "Synthesis and evaluation of antioxidant and antibacterial behavior of CuO nanoparticles", Colloids and Surfaces B: Biointerfaces **101** (2013) 430. https://doi.org/10.1016/j.colsurfb.2012.07.002.

[26] M. Gao, L. Sun, Z. Wang & Y. Zhao, "Controlled synthesis of Ag nanoparticles with different morphologies and their antibacterial properties", Materials Science and Engineering:C **33** (2013) 397. https://doi.org/10.1016/j.msec.2012.09.005.

[27] X. G. Zheng, C. N. Xu, Y. Tomokiyo, E. Tanaka, H. Yamada & Y. Soejima, "Observation of charge stripes in cupric oxide", Physical Review Letters **85** (2000) 5170. https://doi.org/10.1103/PhysRevLett.85.5170.

[28] H. R. Naika, K. Lingaraju, K. Manjunath, D. Kumar, G. Nagaraju, D. Suresh & H. Nagabhushana, "Green synthesis of CuO nanoparticles using Gloriosa superba L. extract and their antibacterial activity", Journal of Taibah University for Science **9** (2015) 7. https://doi.org/10.1016/j.jtusci.2014.04.006.

[29] K. Velsankar, R.M. Aswin Kumara, R. Preethi, V. Muthulakshmi & S. Sudhahar, "Green synthesis of CuO nanoparticles via Allium sativum extract and its characterizations on antimicrobial, antioxidant, antilarvicidal activities", Journal of Environmental Chemical Engineering **8** (2020) 104123. https://doi.org/10.1016/j.jece.2020.104123.

[30] H.N. Jayasimha, K.G. Chandrappa, P.F. Sanaulla & V.G. Dileepkumar, "Green synthesis of CuO nanoparticles: A promising material for photocatalysis and electrochemical sensor", Sensors International **5** (2024) 100254. https://doi.org/10.1016/j.sintl.2023.100254.

[31] S.A. Akintelu, A.S. Folorunso, F.A. Folorunso & A.K. Oyebamiji, "Green synthesis of copper oxide nanoparticles for biomedical application and environmental remediation" , Heliyon **6** (2020) e04508. https://doi.org/10.1016/j.heliyon.2020.e04508.

[32] V.V.T. Padil & M. Černík, "Green synthesis of copper oxide nanoparticles using gum karaya as a biotemplate and their antibacterial application", International Journal of Nanomedicine 8**8** (2013) 889. https://doi.org/10.2147/IJN.S40599.

[33] S. Nouren, I. Bibi, A. Kausar, M. Sultan, H. Nawaz Bhatti, Y. Safa, S. Sadaf, N. Alwadai & M. Iqbal, "Green synthesis of CuO nanoparticles using Jasmin sambac extract: Conditions optimization and photocatalytic degradation of Methylene Blue dye", Journal of King Saud University-Science **36** (2024) 103089. https://doi.org/10.1016/j.jksus.2024.103089.

[34] Z. Alhalili, "Green synthesis of copper oxide nanoparticles CuO NPs from Eucalyptus Globoulus leaf extract: Adsorption and design of experiments", Arabian Journal of Chemistry **15** (2022) 103739. https://doi.org/10.1016/j.arabjc.2022.103739.

[35] L. G. Prasad, R. Ravikumar, R. G. Raman & R. R. Kanna, "Investigations on the structural, vibrational, optical and photocatalytic behavior of CuO, MnO and CuMnO nanomaterials", Journal of the Nigerian Society of Physical Sciences **6** (2024) 2137. https://doi.org/10.46481/jnsps.2024.2137.

[36] J. K. Sharma, M. S. Akhtar, S. Ameen, P. Srivastava & G. Singh, "Green synthesis of CuO nanoparticles with leaf extract of Calotropis gigantea and its dye-sensitized solar cells applications", Journal of Alloys and Compounds **632** (2015) 321. https://doi.org/10.1016/j.jallcom.2015.01.172.

[37] B. H. Akpeji, B. Lari, U. A. Igbuku, G. Tesi, E. E. Elemike & P. O. Akusu, "Synthesis and characterization of MnO2 nanoparticles mediated by Raphia hookeri seed", Journal of the Nigerian Society of Physical Sciences **6** (2024) 2203. https://doi.org/10.46481/jnsps.2024.2203.

[38] P. P. N. V. Kumar, U. Shameem, P. Kollu, R. L. Kalyani & S. V. N. Pammi, "Green synthesis of copper oxide nanoparticles using Aloe vera leaf extract and its antibacterial activity against fish bacterial pathogens", Bio-NanoScience **5** (2015) 135. https://doi.org/10.1007/s12668-015-0171-z.

[39] K. H. Hassan, A. A. Jarullah, S .K. Saadi & P. Harris, "Green synthesis and structural characterisation of CuO nanoparticles prepared by using fig leaves extract", Pakistan Journal of Scientific & Industrial Research Series A: Physical Sciences **61** (2018) 59. https://doi.org/10.52763/pjsir.phys.sci.61.2.2018.59.65.

[40] M. Gowri, N. Latha & M. Rajan, "Copper oxide nanoparticles synthesized using Eupatorium odoratum, Acanthospermum hispidum leaf extracts, and its antibacterial effects against pathogens: a comparative study", BioNanoScience **9** (2019) 545. https://doi.org/10.1007/s12668-019-00655-7.

[41] N. Al-Qasmi, "Facial eco-friendly synthesis of copper oxide nanoparticles using chia seeds extract and evaluation of its electrochemical activity", Processes **9** (2021) 2027. https://doi.org/10.3390/pr9112027.

[42] M. Yadav, S. Jain, R. Tomar, G. B. K. S. Prasad & H. Yadav, "Medicinal and biological potential of pumpkin: An updated review", Nutrition Research Reviews **23** (2010) 184. https://doi.org/10.1017/S0954422410000107.

[43] E. P. Mukhokosi, M. Maaza, M. Tibenkana, N. L. Botha, L. Namanya, I. G. Madiba & M. Okullo, "Optical absorption and photoluminescence properties of Cucurbita maxima dye adsorption on TiO2 nanoparticles", Materials Research Express **10** (2023) 046203. https://doi.org/10.1088/2053-1591/acce91.

[44] E. P. Mukhokosi, T. Mohammed, N. Loyce, N. L. Botha, M. Maaza & D. Velauthapillai, "Co-sensitization effect of chlorophyll and anthocyanin on optical absorption properties and power conversion efficiency of dye-sensitized solar cells", Journal of the Korean Physical Society **84** (2024) 858. https://doi.org/10.1007/s40042-024-01070-2.

[45] M. D. Tyona, "A theoritical study on spin coating technique", Advances in Materials Research **2** (2013) 195. https://doi.org/10.12989/amr.2013.2.4.195.

[46] S. J. Kim, J. H. We, J. S. Kim, G. S. Kim & B. J. Cho, "Thermoelectric properties of P-type Sb2Te3 thick film processed by a screen-printing technique and a subsequent annealing process", Journal of alloys and compounds **582** (2014) 177. https://doi.org/10.1016/j.jallcom.2013.07.195.

[47] S. Sathyajothi, R. Jayavel & A.C. Dhanemozhi, "The fabrication of natural dye sensitized solar cell (Dssc) based on TiO2 using Henna and Beetroot dye extracts", Materials Today: Proceedings **4** (2017) 668. https://doi.org/10.1016/j.matpr.2017.01.071.

[48] G .W. Mukwaya, B. Enjiku & E. P. Mukhokosi, "Structural and mechanical properties of non-glazed ceramic tiles developed from selected mineral deposits in Uganda", Nano-Horizons: Journal of Nanosciences and Nanotechnologies **2** (2023) 14. https://doi.org/doi.org/10.25159/NanoHorizons/13816.

[49] T. S. Aldeen, H. E. Ahmed Mohamed & M. Maaza, "ZnO nanoparticles prepared via a green synthesis approach: Physical properties, photocatalytic and antibacterial activity", Journal of Physics and Chemistry of Solids **160** (2022) 110313. https://doi.org/10.1016/j.jpcs.2021.110313.

[50] W .W. Andualem, F. K. Sabir, E.T. Mohammed, H. H. Belay & B. A. Gonfa, "Synthesis of copper oxide nanoparticles using plant leaf extract of catha edulis and its antibacterial activity", Journal of Nanotechnology **2020** (2020) 2932434. https://doi.org/10.1155/2020/2932434.

[51] W. Hou & S. B. Cronin, "A review of surface plasmon resonance-enhanced photocatalysis", Advanced Functional Materials **23** (2013) 1612. https://doi.org/10.1002/adfm.201202148.

[52] R. W. Johns, H. A. Bechtel, E. L. Runnerstrom, A. Agrawal, S. D. Lounis & D. J. Milliron, "Direct observation of narrow mid-infrared plasmon linewidths of single metal oxide nanocrystals", Nature Communications **7** (2016) 11583. https://doi.org/10.1038/ncomms11583.

[53] E. P. Mukhokosi, S. B. Krupanidhi & K. K. Nanda, "Band gap engineering of hexagonal SnSe2 nanostructured thin films for infra-red photodetection", Scientific reports **7** (2017) 15215. https://doi.org/10.1038/s41598-017-15519-x.

[54] V. Solanki, S. Majumder, I. Mishra, S. R. Joshi , D. Kanjilal & S. Varma, "Size-dependent optical properties of TiO2 nanostructures", Radiation Effects and Defects in Solids **168** (2013) 518. https://doi.org/10.1080/10420150.2013.777444.

[55] R. Article, M. U. Khan, S. Honey, M. Abbas, T. Ahmad, A. Sohail, J. Ahmad, H. Ullah, Z. Talib, A. Umar, J. Sohail, K. Makgopa & J. Asim, "Metal nanoparticles : Synthesis approach , types and applications – a mini review", Journal of Nanosciences and Nanotechnologies **2** (2023) 21. https://doi.org/doi.org/10.25159/NanoHorizons.87a973477e35.

[56] M. Malik, M. Henini, F. Ezema, E. Manikandan, J. Kennedy, K. Bouziane, M. Chaker, A. Gibaud, A.K.F. Haque, Z. Nuru, I. Ahmad, R. Obodo & M. Akbari, "Peculiar size effects in nanoscaled systems", Journal of Nanosciences and Nanotechnologies **1** (2022) 36. https://doi.org/10.25159/nanohorizons.9d53e2220e31.

[57] P. K. Raul, S. Senapati, A. K. Sahoo, I. M. Umlong, R. R. Devi, A. J. Thakur & V. Veer, "CuO nanorods: A potential and efficient adsorbent in water purification", RSC Advances **4** (2014) 40580. https://doi.org/10.1039/c4ra04619f.

[58] K. Vishveshvar, M. V. Aravind Krishnan, K. Haribabu & S. Vishnuprasad, "Green synthesis of copper oxide nanoparticles using Ixiro coccinea plant leaves and its characterization", BioNanoScience **8** (2018) 554. https://doi.org/10.1007/s12668-018-0508-5.

[59] R. Sathyamoorthy & K. Mageshwari, "Synthesis of hierarchical CuO microspheres: Photocatalytic and antibacterial activities", Physica E: Low-dimensional Systems and Nanostructures **47** (2013) 157. https://doi.org/10.1016/j.physe.2012.10.019.

[60] A. H. Alami, B. Rajab, J. Abed, M. Faraj, A. A. Hawili & H. Alawadhi, "Investigating various copper oxides-based counter electrodes for dye sensitized solar cell applications", Energy **174** (2019) 526. https://doi.org/10.1016/j.energy.2019.03.011.

[61] L. Wang, Y. Shi, H. Zhang, X. Bai, Y. Wang & T. Ma, "Iron oxide nanostructures as highly efficient heterogeneous catalysts for mesoscopic photovoltaics", Journal of Materials Chemistry A **2** (2014) 15279. https://doi.org/10.1039/c4ta03727h.

[62] M. Wu, X. Lin, A. Hagfeldt & T. Ma, "A novel catalyst of WO2 nanorod for the counter electrode of dye-sensitized solar cells", Chemical Communications **57** (2011) 4535. https://doi.org/10.1039/c1cc10638d.

[63] G. R. Mutta, S. R. Popuri, J. I. B. Wilson & N. S. Bennett, "Sol-gel spin coated well adhered MoO3 thin films as an alternative counter electrode for dye sensitized solar cells", Solid State Sciences **61** (2016) 84. https://doi.org/10.1016/j.solidstatesciences.2016.08.016.

[64] C. H. Tsai, P. H. Fei, C. M. Lin & S. L. Shiu, "CuO and CuO/graphene nanostructured thin films as counter electrodes for Pt-free dye-sensitized solar cells", Coatings **8** (2018) 21. https://doi.org/10.3390/

coatings8010021.

[65] J. C. Morka, I. E. Ottih & N. S. Umeokwonna, "Growth and characterization of dye-sensitized solar cells using dyes from Mangifera indica, Manihot esculenta and Hibiscus sabdariffa leaves by sol-gel technique", Journal of Applied Sciences and Environmental Managemen **26** (2022) 1785. https://doi.org/10.4314/jasem.v26i11.8.

[66] G. Richhariya, A. Kumar, P. Tekasakul & B. Gupta, "Natural dyes for dye sensitized solar cell: A review", Renewable and Sustainable Energy Reviews **69** (2017) 705. https://doi.org/10.1016/j.rser.2016.11.198.

[67] J. Gong, K. Sumathy, Q. Qiao & Z. Zhou, "Review on dye-sensitized solar cells (DSSCs): Advanced techniques and research trends", Renewable and Sustainable Energy Reviews **68** (2017) 234. https://doi.org/10.1016/j.rser.2016.09.097.

[68] G. F. C. Mejica, Y. Unpaprom & R. Ramaraj, "Fabrication and performance evaluation of dye-sensitized solar cell integrated with natural dye from Strobilanthes cusia under different counter-electrode materials", Applied Nanoscience **13** (2023) 1073. https://doi.org/10.1007/s13204-021-01853-0.

[69] D. Eli, P. M. Gyuk & E. Danladi, "Chlorophyll and betalain as light-harvesting pigments for nanostructured TiO2 based dye-sensitized solar cells", Journal of Energy and Natural Resources **5** (2016) 53. https://doi.org/10.11648/j.jenr.20160505.11.

[70] D. D. Pratiwi, F. Nurosyid, A. Supriyanto & R. Suryana, "Optical properties of natural dyes on the dye-sensitized solar cells (DSSC) performance", Journal of physics: Conference series **776** (2016) 012007. https://doi.org/10.1088/1742-6596/776/1/012007.

[71] M. K. Hossain, M. F. Pervez, M. N. H. Mia, A. A. Mortuza, M. S. Rahaman, M. R. Karim, J. M. M. Islam, F. Ahmed & M. A. Khan, "Effect of dye extracting solvents and sensitization time on photovoltaic performance of natural dye sensitized solar cells", Results in Physics **7** (2017) 1516. https://doi.org/10.1016/j.rinp.2017.04.011.